

## Effects of Sn-Ag-x layers on the solderability and mechanical properties of Sn-58Bi solder

Zhang, Shuang; Liu, Yang; Zhang, Hao; Zhou, Min; Xue, Yuxiong; Zeng, Xianghua; Cao, Rongxing; Chen, Penghui

**DOI**

[10.1080/09507116.2021.1913451](https://doi.org/10.1080/09507116.2021.1913451)

**Publication date**

2021

**Document Version**

Final published version

**Published in**

Welding International

**Citation (APA)**

Zhang, S., Liu, Y., Zhang, H., Zhou, M., Xue, Y., Zeng, X., Cao, R., & Chen, P. (2021). Effects of Sn-Ag-x layers on the solderability and mechanical properties of Sn-58Bi solder. *Welding International*, 35(1-3), 16-23. <https://doi.org/10.1080/09507116.2021.1913451>

**Important note**

To cite this publication, please use the final published version (if applicable).  
Please check the document version above.

**Copyright**

Other than for strictly personal use, it is not permitted to download, forward or distribute the text or part of it, without the consent of the author(s) and/or copyright holder(s), unless the work is under an open content license such as Creative Commons.

**Takedown policy**

Please contact us and provide details if you believe this document breaches copyrights.  
We will remove access to the work immediately and investigate your claim.



## Effects of Sn-Ag-x layers on the solderability and mechanical properties of Sn-58Bi solder

Shuang Zhang, Yang Liu, Hao Zhang, Min Zhou, Yuxiong Xue, Xianghua Zeng, Rongxing Cao & Penghui Chen

To cite this article: Shuang Zhang, Yang Liu, Hao Zhang, Min Zhou, Yuxiong Xue, Xianghua Zeng, Rongxing Cao & Penghui Chen (2021): Effects of Sn-Ag-x layers on the solderability and mechanical properties of Sn-58Bi solder, *Welding International*, DOI: [10.1080/09507116.2021.1913451](https://doi.org/10.1080/09507116.2021.1913451)

To link to this article: <https://doi.org/10.1080/09507116.2021.1913451>



Published online: 19 Apr 2021.



Submit your article to this journal [↗](#)



Article views: 13



View related articles [↗](#)



View Crossmark data [↗](#)



## Effects of Sn-Ag-x layers on the solderability and mechanical properties of Sn-58Bi solder

Shuang Zhang<sup>a,b</sup>, Yang Liu<sup>b</sup>, Hao Zhang<sup>c</sup>, Min Zhou<sup>b</sup>, Yuxiong Xue<sup>b</sup>, Xianghua Zeng<sup>b</sup>, Rongxing Cao<sup>b</sup> and Penghui Chen<sup>b</sup>

<sup>a</sup>School of Material Science and Engineering, Harbin University of Science and Technology, Harbin, China; <sup>b</sup>College of Electrical, Energy and Power Engineering, Yangzhou University, Yangzhou, China; <sup>c</sup>Department of Microelectronics, Delft University of Technology, Delft, The Netherlands

### ABSTRACT

Sn-Ag-x solders were used as the interfacial layers between SnBi solder and Cu substrate. The effects of Sn-Ag-x layers on the solderability, microstructure, and mechanical properties of SnBi solder joint were investigated. Experimental results indicate that all the barrier layers have positive effects on improving the wettability of SnBi solder. The relative area and grain size of  $\beta$ -Sn was enlarged due to the addition of Sn-Ag-x layers. Meanwhile, the addition of the interfacial layers decreased the hardness of the SnBi solder joint. The addition of Sn-Ag-x layers increased the thickness of the interfacial intermetallic compound (IMC) but had limited effects on the shear force of the SnBi solder joint. Due to the addition of the interfacial layers, the brittleness of the SnBi/Cu solder joints during the shear test was slightly suppressed.

### ARTICLE HISTORY

Received 04 February 2021  
Accepted 02 April 2021

### KEYWORDS

Interfacial layers; SnBi; microstructure; hardness; shear behaviour

## 1. Introduction

Modern electronic equipment is developing towards lightweight and high integration, which puts forward higher requirements for packaging materials and structures. The life of electronic equipment usually depends on the quality of the solder joints. With the development of lead-free soldering technology in recent years, SnBi solder has attracted attention due to its low melting temperature, low cost and wide usage in the field of low-temperature soldering [1,2]. However, because the SnBi alloy contains a large amount of coarse Bi-rich phases, the plasticity of the solder joints deteriorates. In addition, the wettability and thermal conductivity of SnBi solder are also important aspects to be improved.

Adding trace elements is the common method to improve the microstructure and property of the SnBi solder alloy. Yang et al. [3] introduced that the microstructure of SnBi solder was refined with the addition of 0.25 wt.% Mo. The failure mode of SnBi-0.25Mo solder joints changed from brittle fracture to mixed fracture. Mokhtari et al. [4] found that adding a small amount of In or Ni elements into SnBi solder effectively suppressed the growth of the interfacial IMC and the coarsening of Bi-rich phase during the isothermal ageing treatment. Chen et al. [5] found that the elongation of Sn-Bi solder was increased by 44.5% after adding

2.5% In element. Additionally, as indicated by Wang et al. [6], the addition of In element could effectively reduce the melting point of the solder and improve the wettability. Wu et al. [7] added Cu into the SnBi solder paste. The results showed that an appropriate amount of Cu element refined the structure and increased the ultimate tensile strength of the SnBi solder alloy. Myung et al. [8] studied the addition of Ag into SnBi solders, and the results showed that the shear strength of the solder joint was improved after adding 1 wt.% Ag.

Another way to improve the soldering quality of SnBi solder is to add coating layers on the soldering substrates. Sn-Ag-x solders, such as Sn-Ag-Cu, show better ductility and thermal ageing resistance than SnBi does. Therefore, such solders are considered as the interfacial layers between SnBi and pad materials [9]. Wang et al. [10] obtained a 5  $\mu\text{m}$ -thick SnAgCu coating on the surface of Cu substrate by Hot Air Soldering Levelling (HASL) method, which effectively inhibited the growth of the intermetallic compound (IMC) layer on the interface of SnBi/Cu solder joints during ageing. Liu et al. [11] adopted the SAC305 solder balls to form the SnBi/SAC305/Cu composite structure. The results showed that SAC305 bumps had positive effects on suppressing the brittle failure of the SnBi solder joints.

In this work, four kinds of Sn-Ag-x solder layers were coated on Cu pads. The solderability,

microstructure, and mechanical properties of the SnBi/Sn-Ag-x/Cu solder joints were investigated.

## 2. Experimental procedure

The solder materials used in this work were commercial Sn-3.0Ag-0.5Cu (SAC305), Sn-0.3Ag-0.7Cu (SAC0307), Sn-0.3Ag-0.7Cu-0.5Bi-Ni (SACBN), Sn-3.0Ag-3.0Bi-3.0In (SABI333), Sn-58Bi (SnBi) solder pastes. The substrates were Cu pads with an open diameter of 640  $\mu\text{m}$  on the PCB. Firstly, a small amount of the SAC305, SAC0307, SACBN and SABI333 solder pastes were soldered onto the Cu pads, respectively. The parts higher than the solder barrier layer were grinded with sandpaper. Figure 1 shows the structure of the barrier layer formed by SAC305 solder after the above treatment. The structures of the barrier layer of the other three solders, SAC0307, SACBN, and SABI333 are the same as shown in Figure 1, among which the soldering temperature of SAC305, SAC0307, SACBN onto the Cu pads was 260°C. The soldering temperature of SABI333 solder onto the Cu pads was 230°C, and the time was 80s. Secondly, the SnBi solder paste

was dispensed onto the barrier layer by the Create-PSD solder paste dispenser. Then, the samples were soldered at 180°C for 80s to form the solder joints. The schematic diagram of manufacturing this structure is shown in Figure 2. For comparison, the pure SnBi/Cu solder joint was also soldered at 180°C for 80s. Here, the height of the five kinds of solder joints was about 610  $\mu\text{m}$ .

The as-soldered samples were cross-sectioned by grinding and polishing. The microstructure and chemical composition of the solder joint were characterized by scanning electron microscopy (SEM) and energy-dispersive spectrum (EDS). In order to study the impact of the barrier layer on the mechanical properties of SnBi solder, the shear force of solder joints was obtained by RESCH PTR-1100 tester. Here the shear height was set as 45  $\mu\text{m}$ , and the shear speed was set as 0.02 mm/s. The hardness of solder joints was obtained by SHIMADZU DUH-211S nanoindentation tester. The test force was 20 mN and the loading speed was 5 mN/s. The Poisson's ratio of SnBi solder was 0.35. The fracture morphologies were observed by SEM. According to the Japanese Industrial Standard JIS-Z3197, the

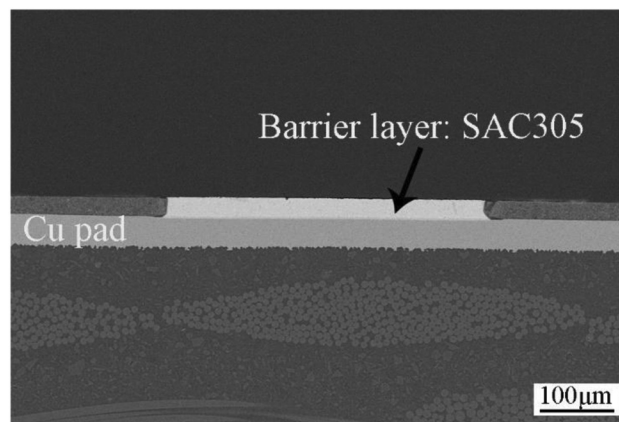


Figure 1. The structure of the barrier layer formed by the SAC305 solder paste.

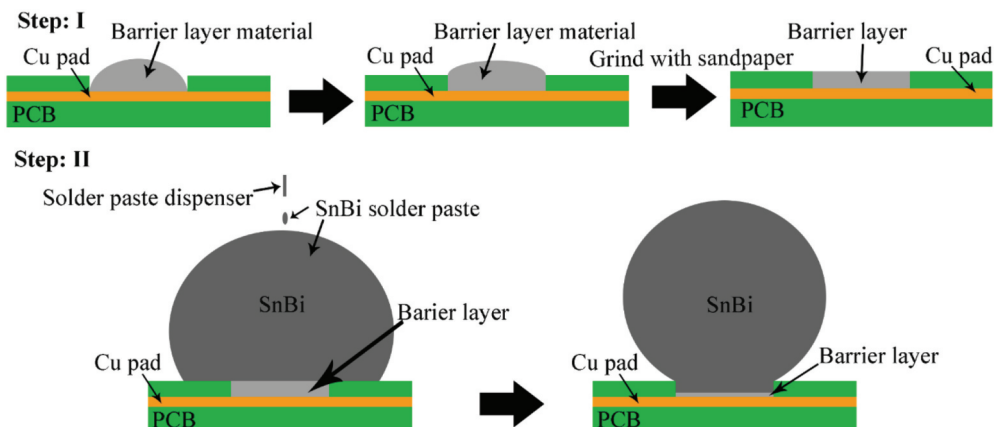


Figure 2. Manufacturing process and schematic diagram of the solder joint with barrier layer.

spread coefficient  $K$  was used to evaluate the wettability of the SnBi solder on SAC305, SAC0307, SACBN, and SABI333 solders.  $K$  was defined as follows:

$$K = \frac{D - H}{D} \times 100\% \quad (1)$$

Where  $K$  was the spreading coefficient (%),  $H$  was the height after solder spreading (mm), and  $D$  was the diameter of a sphere equal to the volume of solder (mm).

### 3. Results and discussion

#### 3.1. Wettability

Wettability is one of the important characteristics to evaluate the solderability of the lead-free solder [12]. In this study, the wettability of SnBi solder on barrier layer is evaluated by spreading coefficient. The calculation method is shown in Equation (1). The spreading coefficient of the SnBi solder on barrier layer is shown in Figure 3. The experimental results are the average values of the five tests of each sample, which are larger than that on the Cu substrate. The spreading coefficient of SnBi on the SAC305 and SAC0307 barrier layers increases by 6.2% compared to that on the Cu pad, from 0.81 to 0.86. The spreading coefficient on the SACBN barrier layer reaches 0.87. The spreading coefficient of SnBi on the SABI333 barrier layer is 0.89, which is the largest spreading coefficient. The wettability of the SnBi solder on the barrier layer is better than that on the Cu board. The reason may be that the barrier layer is Sn-based solder. The Sn element diffuses into the liquid SnBi solder during the heating process, thus reducing the interface energy between the solder and the barrier layer to reduce the surface tension. In addition, Bi is a surface-active element [13]. It can reduce the surface tension of liquid solder and

promote the spread of the solder on substrate. The surface-active element Bi exists in the two barrier layers of SACBN and SABI333 and further reduces the surface tension, so the wettability is relatively good.

#### 3.2. Microstructure of solder joints

Figure 4(a–e) shows the SEM microstructures of the Sn-Bi bulk solder in the five types of the solder joints. The SnBi/Cu solder joints have a typical eutectic structure. The bright area is the Bi-rich phase, and the dark area is the Sn-rich phase, as shown in Figure 4(a). This is consistent with the previous researches [14,15]. From the Figure 4(b–e) of SnBi/SAC305/Cu, SnBi/SAC0307/Cu, SnBi/SACBN/Cu, SnBi/SABI333/Cu solder joints, it can be observed that the structures formed by the four solder joints are similar, which are composed of two parts: eutectic structure and quasi-peritectic structures (the parts are circled in red). Each part contains Sn-rich phase and Bi-rich phase. The formation of these two parts can be explained by the Sn-Bi binary eutectic phase diagram. There are two reactions during the heating process. One is the eutectic reaction  $L \rightarrow Sn + Bi$  that occurs at the eutectic point. The other is  $L + \beta \rightarrow Sn + Bi$  during which the Sn element in the barrier layer dissolves into the molten SnBi solder, so the microstructure changes in the hypoeutectic zone. There are more quasi-peritectic structures in Figure 4(b–e) compared with the typical Sn-58Bi eutectic structure. At the same time, it can be clearly found that the structures in Figure 4(b–e) are thicker than that in Figure 4(a), and the  $\beta$ -Sn and Bi phases are larger in size. Figure 4(f) is the EDS result of the corresponding point in Figure 4(a). The Ag, Cu and other elements form the intermetallic compound  $Ag_3Sn$ ,  $Cu_6Sn_5$  and other second-phase particles in the microstructure. The second-phase particles act as heterogeneous

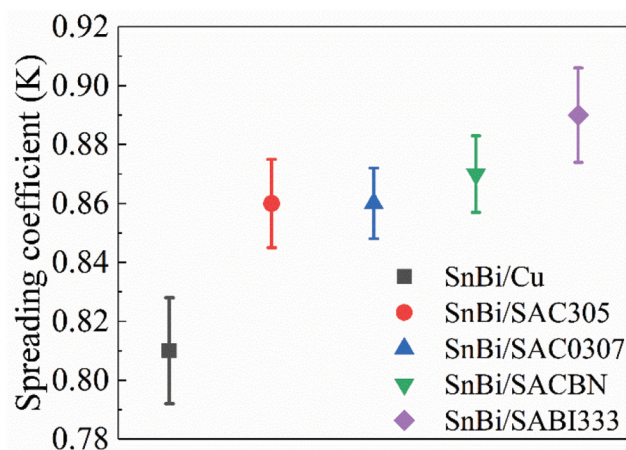
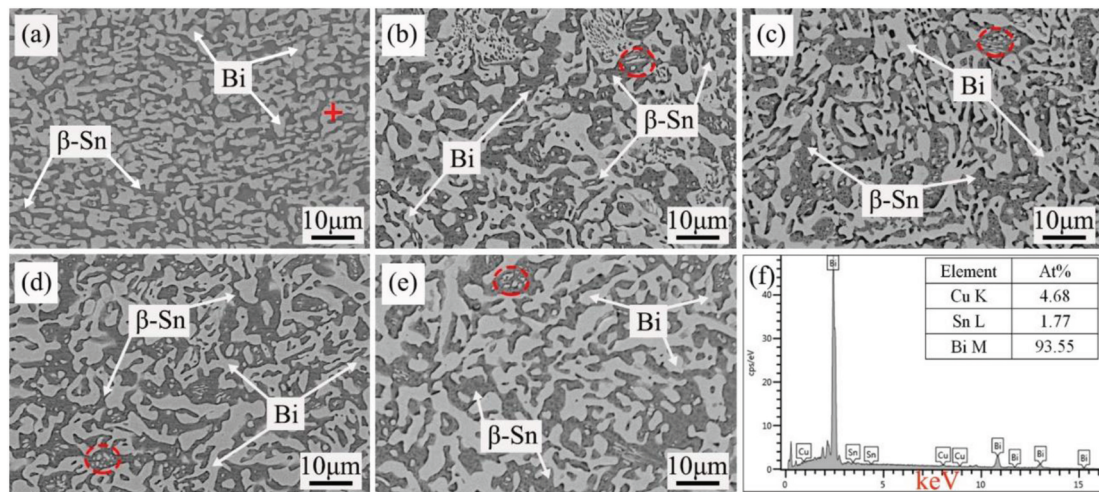


Figure 3. Effects of the barrier layer on the spreadability of SnBi solder.



**Figure 4.** SEM microstructures of SnBi solder on the bare Cu pad (a) and on the SAC305, SAC0307, SACBN, SABI333 barrier layer (b–e), (f) EDS of the point in (a).

nucleation points and accelerate the nucleation rate during the cooling and solidification process. However, the Bi particles attached to these particles have no time to diffuse from  $\beta$ -Sn. Thus, there are some quasi-peritectic structures in Figure 4(b–e).

The interface microstructures of SnBi solder on the bare Cu substrate and the Sn–Ag–x barrier layer are shown in Figure 5. Figure 5(a) shows the SnBi/Cu solder joint. The solder part has a typical SnBi eutectic structure, and a compound is formed at the interface as a connection. The interfacial IMC formed by SnBi/Cu solder joint is  $\text{Cu}_6\text{Sn}_5$  according to the reported work [16]. This study obtains the same result, as shown in Table 1. Due to the high content of Bi in the solder, a large number of Bi blocks form in the solder joint and cover on  $\text{Cu}_6\text{Sn}_5$ . The IMC exhibits thin and flat morphology due to the growth inhibition. At the interface, the pre-prepared barrier layer completely dissolves into

the SnBi solder (Figure 5(b–e)), and a thicker IMC layer can be observed between the solder and the Cu pad. Figure 5(f) shows that the IMC composition in Figure 5(d) is  $(\text{Cu}, \text{Ni})_6\text{Sn}_5$ . Table 1 shows the EDS results of points 1, 2, 3, 4, and 5 in Figure 5. It can be seen that except that the SnBi/SACBN/Cu solder joint interface IMC forms  $(\text{Cu}, \text{Ni})_6\text{Sn}_5$ , the composition of the other four solder joint interface IMCs are all  $\text{Cu}_6\text{Sn}_5$ . The growth of  $\text{Cu}_6\text{Sn}_5$  at the interface can be expressed by the following reaction:



The formation of  $\text{Cu}_6\text{Sn}_5$  is usually formed by a chemical reaction between Sn atoms in the molten solder and Cu atoms in the Cu substrate. It plays an important role in  $\text{Cu}_6\text{Sn}_5$  IMC formation and growth [17]. During the subsequent heating process, the grain boundaries between  $\text{Cu}_6\text{Sn}_5$  as diffusion channels are used by the Cu atoms in the Cu substrate, and diffuse

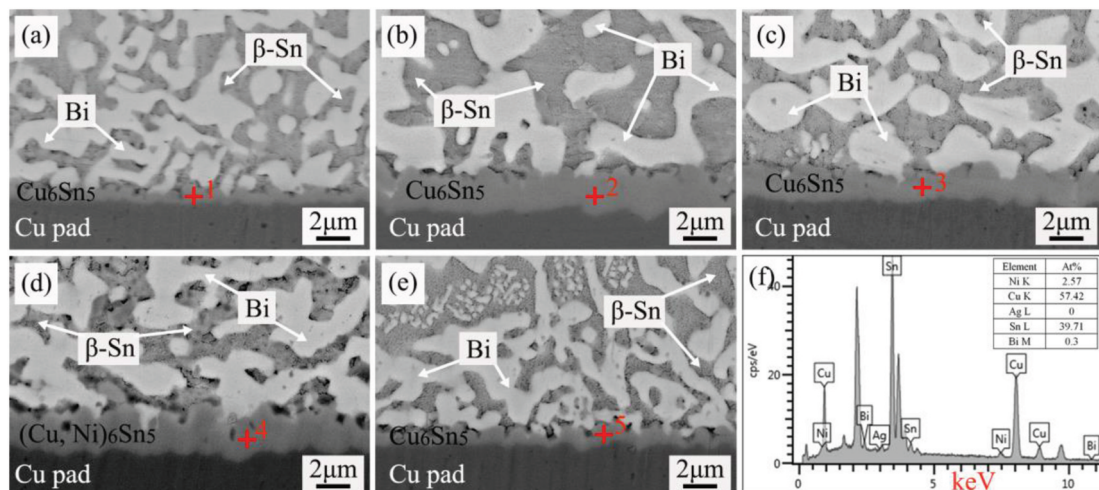


**Figure 5.** Interfacial structures of Sn–58Bi solder on the bare Cu pad (a) and on the SAC305, SAC0307, SACBN, SABI333 barrier layers (b–e), (f) EDS of the point 4.

**Table 1.** EDS analysis results of different point in Figure 5.

Point	At%					
	Sn	Cu	Bi	Ag	In	Ni
Point 1	48.22	51.38	0.4	/	/	/
Point 2	44.47	54.89	0.42	0.22	/	/
Point 3	42.65	57	0.35	0	/	/
Point 4	39.71	57.42	0.3	0	/	2.57
Point 5	47.96	51.26	0.62	0.02	0.14	/

into the liquid solder and react with the Sn atoms in the solder, thereby thickening the  $\text{Cu}_6\text{Sn}_5$  IMC. Therefore, the reason why the IMC of the four solder joints of SnBi/SAC305/Cu, SnBi/SAC0307/Cu, SnBi/SACBN/Cu, SnBi/SABI333/Cu is thicker than that of the IMC of the SnBi/Cu solder joint can be explained as  $\text{Cu}_6\text{Sn}_5$  or  $(\text{Cu}, \text{Ni})_6\text{Sn}_5$  has been formed at the interface when preparing the barrier layer. During the second soldering process, the barrier layers dissolve into the liquid SnBi solder. When the liquid solder contacts the  $\text{Cu}_6\text{Sn}_5$  or  $(\text{Cu}, \text{Ni})_6\text{Sn}_5$  IMC layer generated during the first soldering process, the Sn atoms in the solder directly react with the Cu atoms diffused through the  $\text{Cu}_6\text{Sn}_5$  or  $(\text{Cu}, \text{Ni})_6\text{Sn}_5$  grain boundaries in the Cu pad, resulting in the thickening of IMC. The inconsistent growth of the IMC thickness may be due to the difference in the particle size of the IMC generated during the first soldering, resulting in the difference in the number of grain boundaries, thereby affecting the diffusion flux of Cu atoms.

### 3.3. Hardness and shear behaviour on solder joints

The nanoindentation is a common method to test the hardness of solder joints [18,19]. The nanoindentation experiment is used to test the hardness of the solder in the five solder joints, and the results are shown in Figure 6. Figure 6(a) shows the load–depth relationship of the composite solder joints. It can be seen from

the curve that the depth of the indentation increases with the increase in the loading force. Under the test conditions, the indentation depth of the bulk solder of the SnBi/Cu solder joint is about 1.4  $\mu\text{m}$ . This depth is the smallest of all the tested solder joints. After adding a barrier layer to the SnBi/Cu interface, the solder indentation depth of the solder joint body increases to varying degrees, among which SnBi/SAC0307/Cu solder joints have the largest indentation depth of bulk solder.

Figure 6(b) shows the influence of the barrier layer on the hardness of SnBi solder. The average hardness of the bulk solder of the SnBi/Cu solder joint is 357.6MPa, which is significantly higher than the average hardness of the solder joint after adding a barrier layer. According to reference [18], the hardness of the pure SnBi solder is about 166.5MPa. The hardness tested in this paper is higher than this value. This is due to the continuous diffusion of Cu on the substrate into the SnBi solder bulk during the soldering process. Therefore, the hardness of the SnBi solder bulk increases. In particular, the average hardness of the bulk solder of the SnBi/SAC0307/Cu solder joint is 255.1MPa. Compared with SnBi/Cu solder joints, the hardness of bulk solder has decreased by 28.7%, which is the lowest among the five solder joints. In addition, the bulk solder hardness of SnBi/SACBN/Cu solder joints and SnBi/SABI333/Cu solder joints is higher than that of SnBi/SAC0307/Cu solder joints and SnBi/SAC305/Cu solder joints. From the microstructure of the solder joints, it can be seen that with the addition of barrier layers at the interface of SnBi/Cu, the Sn concentration,  $\beta$ -Sn, and Bi phase sizes increase in the SnBi block. The increase of  $\beta$ -Sn size is the main factor leading to the decrease in solder hardness [20,21]. In SnBi/SACBN/Cu solder joints and SnBi/SABI333/Cu solder joints, because the barrier layer is dissolved into the SnBi solder during the heating

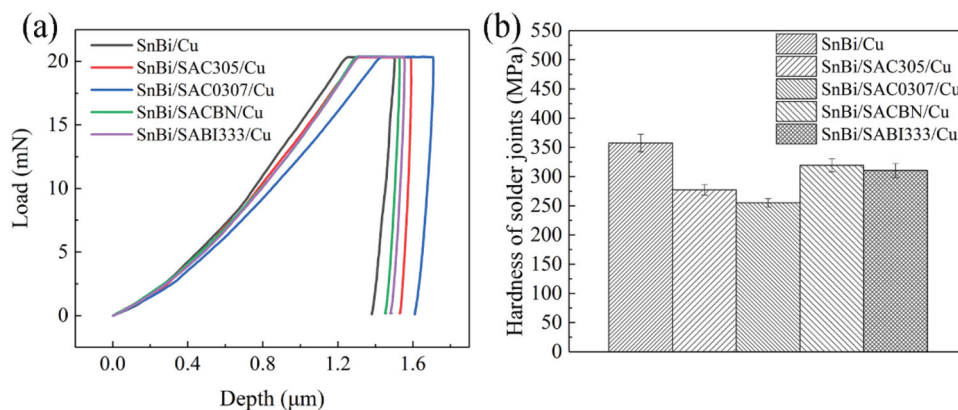


**Figure 6.** Results of the hardness test (a) hardness curves of the five kinds of solder joints. (b) hardness of the five kinds of solder joints.

process, the Bi, Ag, Ni, and In elements diffuse into the solder, and form the second-phase particles, which is considered as the solder joint body the main reason for the increase in the hardness of the solder.

In order to study the influence of the barrier layer on the shear performance of SnBi solder, the ball shear test method is used to evaluate the shear force of SnBi solder. The results are shown in Figure 7. Figure 7(a) shows the comparison of the shear force of SnBi solder on different barrier layers. It can be seen that the shear forces of several solder joints are similar. Therefore, the addition of barrier layer has no obvious effects on the shear force of SnBi solder. Figure 7(b–f) is the force–distance relationship of the five solder joints shear tests of SnBi/Cu, SnBi/SAC305/Cu, SnBi/SAC0307/Cu, SnBi/SACBN/Cu, SnBi/SABI333/Cu. The results show that the shear curves of the five kinds of solder joints are similar, and the shear force decreases sharply after reaching the peak value, and the solder joints show the typical brittle fracture. However, the SnBi/Cu solder shows high shear force. The strengthening phase Bi leads to this result [22]. In addition, by calculating the distance before the solder joint is completely broken, it is found that the complete fracture distance of the SnBi/Cu solder joint is 0.192 mm, which is the smallest of the five solder joints. The complete fracture distance of the solder joints with the barrier layer added is larger than that of the SnBi/Cu solder joints. The SnBi/SACBN/Cu solder joint has the largest fracture distance, which is 0.248 mm. It increases 29.1%.

It is generally believed that the shear force is related to the thickness of the interface IMC [10]. In this

study, the thickness of the interface IMC in the solder joints formed by adding a barrier layer is thicker than that of the interface IMC formed by SnBi solder on bare Cu, as shown in Figure 5(a–e). The shear test results show that there is little difference in the shear force of the five solder joints. For this phenomenon, the possible reason is the  $\text{Cu}_6\text{Sn}_5$  or  $(\text{Cu}, \text{Ni})_6\text{Sn}_5$  crystal grain formed at the interface in the five solder joints. The contact area between the crystal grain and the solder of the SnBi/SAC305/Cu, SnBi/SAC0307/Cu, SnBi/SACBN/Cu, SnBi/SABI333/Cu solder joints are more than SnBi/Cu solder joint. The interface IMC particles are more embedded in solder. It can hinder the movement of dislocations and crack propagation in the bulk solder during the shearing process, which helps to increase the shearing force of the solder joints, thereby making up for the defect that the shearing force is reduced due to the increase of the interface IMC thickness. At the same time, the x element dissolves into SnBi solder, which destroys the original eutectic reaction and forms more quasi-peritectic structures in SnBi solder. It has a positive effect on the shear behaviour of solder joints.

Figure 8 shows the fracture morphologies of solder joints after shear test. The fracture of the SnBi solder joint occurs inside the SnBi solder matrix, as shown in Figure 8(a). The typical layered structure and a large amount of Bi phase of SnBi solder can be seen by observing the local morphology of the fracture, as shown in Figure 8(b). It can be judged that the failure mode of SnBi solder is brittle fracture [23]. Figure 8(c, e, g, i) are the macroscopic fracture shapes of the four solder joints of SnBi/SAC305/Cu, SnBi/SAC0307/Cu,

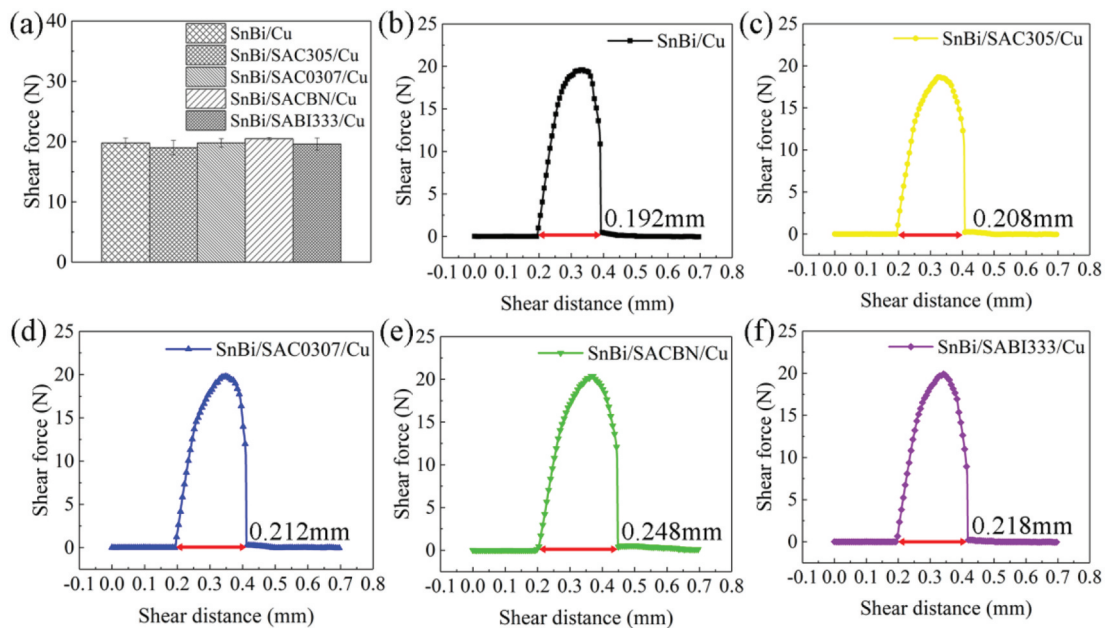
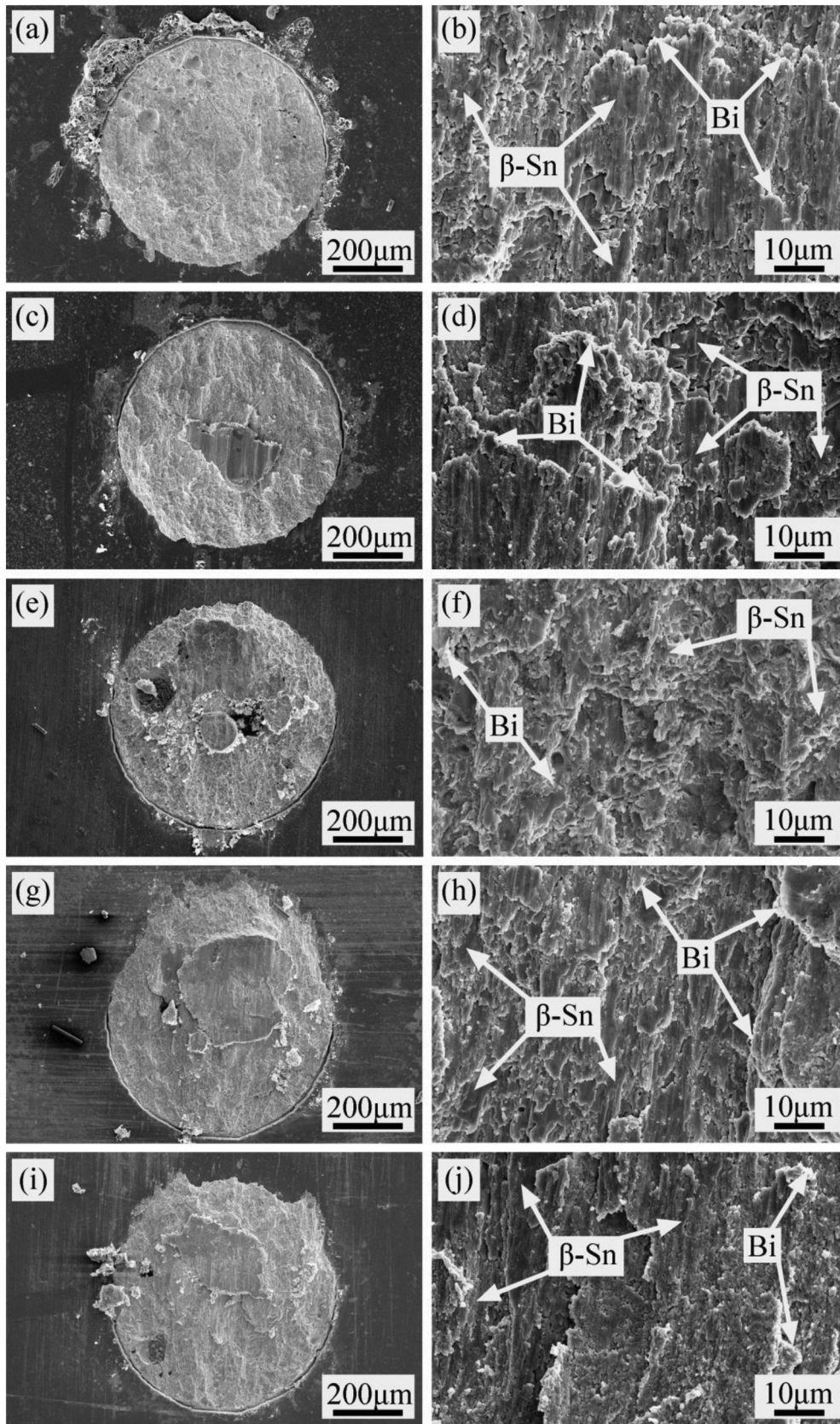


Figure 7. Results of the shear test (a) shear force of the five kinds of solder joints. (b–f) shear curves of SnBi/Cu, SnBi/SAC305/Cu, SnBi/SAC0307/Cu, SnBi/SACBN/Cu, SnBi/SABI333/Cu solder joints.



**Figure 8.** The macroscopic and microscopic fracture morphologies on solder joints: (a,b), SnBi/Cu; (c-d), SnBi/SAC305/Cu; (e,f), SnBi/SAC0307/Cu; (g,h), SnBi/SACBN/Cu; (i,j), SnBi/SABI333/Cu.

SnBi/SACBN/Cu, SnBi/SABI333/Cu appearance. It can be seen that the fracture position is the same with the SnBi/Cu solder joint, and it is still inside the SnBi solder matrix. But the difference is that the solder

residue on the fracture of the solder joint with the barrier layer is more than that of SnBi/Cu solder joint. As shown in the microstructure and shear curve of the solder joints, the addition of the Sn-Ag-x

layers enlarges the  $\beta$ -Sn grains and leads to the increase in shear distance. Therefore, it can be deduced that the addition of the interfacial layers has positive effects on the ductility improvement of the SnBi solder joint.

#### 4. Conclusions

Sn-Ag-x layers were coated on Cu pads and were used as the interfacial layers between SnBi and Cu. The effects of the barrier layer on the wettability, microstructure, interfacial IMC, hardness and shear behaviour of SnBi solder joints were studied.

- (1) The wettability of SnBi on Cu was significantly improved by the addition of Sn-Ag-x layers.
- (2) The composite solder joints showed a larger grain size of  $\beta$ -Sn but lower hardness than the SnBi/Cu joint did.
- (3) The addition of the Sn-Ag-x layers had limited effects on the shear force of SnBi solder joint.
- (4) The addition of the interfacial layers had positive effects on the ductility improvement of the SnBi solder joint.

#### ORCID

Yang Liu  <http://orcid.org/0000-0002-4311-2198>

#### References

- [1] Wang F, Chen H, Huang Y, et al. Recent progress on the development of Sn-Bi based low-temperature Pb-free solders. *J Mater Sci Mater Electron*. 2019;30:3222–3243.
- [2] Goh Y, Hasseb A, Sabri MFM. Effects of hydroquinone and gelatin on the electrodeposition of Sn-Bi low temperature Pb-free solder. *Electricity Act*. 2013;90:265–273.
- [3] Yang L, Zhu L, Zhang Y, et al. Microstructure and reliability of Mo nanoparticle reinforced Sn-58Bi-based lead-free solder joints. *Mater Sci Technol*. 2017;34(8):992–1002.
- [4] Mokhtari O, Nishikawa H. Effects of In and Ni addition on microstructure of Sn-58Bi solder joint. *J Electron Mater*. 2014;43:4158–4170.
- [5] Chen X, Xue F, Zhou J, et al. Effect of In on microstructure, thermodynamic characteristic and mechanical properties of Sn-Bi based lead-free solder. *J Alloys Compd*. 2015;633:377–383.
- [6] Wang Z, Zhang Q, Chen Y, et al. Influences of Ag and In alloying on Sn-Bi eutectic solder and SnBi/Cu solder joints. *J Mater Sci Mater Electron*. 2019;30:18524–18538.
- [7] Wu X, Xia M, Wang X, et al. Microstructure and mechanical behavior of Sn-40Bi-x Cu alloy. *J Mater Sci Mater Electron*. 2017;28:15708–15717.
- [8] Myung W, Ko M, Kim Y, et al. Effects of Ag content on the reliability of LED package component with Sn-Bi-Ag solder. *J Mater Sci Mater Electron*. 2015;26:8707–8713.
- [9] Kariya Y, Otsuka M. Mechanical fatigue characteristics of Sn-3.5Ag-X (X=Bi, Cu, Zn and In) solder alloys. *J Electron Mater*. 1998;27:1229–1235.
- [10] Wang F, Li D, Zhang Z, et al. Improvement on interfacial structure and properties of Sn-58Bi/Cu joint using Sn-3.0 Ag-0.5 Cu solder as barrier. *J Mater Sci Mater Electron*. 2017;28:19051–19060.
- [11] Liu Y, Xu R, Zhang H, et al. Microstructure and shear behavior of solder joint with Sn58Bi/Sn3.0Ag0.5Cu/Cu superposition structure. *J Mater Sci Mater Electron*. 2019;30:14077–14084.
- [12] Dong W, Shi Y, Xia Z, et al. Effects of trace amounts of rare earth additions on microstructure and properties of Sn-Bi-based solder alloy. *J Electron Mater*. 2008;37:982–991.
- [13] Zhou J, Sun Y, Xue F. Properties of low melting point Sn-Zn-Bi solders. *J Alloys Compd*. 2005;397(1–2):260–264.
- [14] Zhang C, Liu S, Qian G, et al. Effect of Sb content on properties of Sn-Bi solders. *Trans Nonferrous Met Soc China*. 2014;24(1):184–191.
- [15] Zhou S, Shen Y, Uresti T, et al. Improved mechanical properties induced by In and In & Zn double additions to eutectic Sn58Bi alloy. *J Mater Sci Mater Electron*. 2019;30:7423–7434.
- [16] Xu R, Liu Y, Zhang H, et al. Evolution of the microstructure of Sn58Bi solder paste with Sn-3.0 Ag-0.5 Cu addition during isothermal aging. *J Electron Mater*. 2019;48:1758–1765.
- [17] Yuan Y, Guan Y, Li D, et al. Investigation of diffusion behavior in Cu-Sn solid state diffusion couples. *J Alloys Compd*. 2016;661:282–293.
- [18] Lv X, He P, Pan F, et al. Effect of Ag nanopowders on microstructure, hardness and elastic modulus of Sn-Bi solders. *Eng Rev*. 2014;34(2):63–68.
- [19] Marques VMF, Johnston C, Grant PS. Nanomechanical characterization of Sn-Ag-Cu/Cu joints—part 1: Young's modulus, hardness and deformation mechanisms as a function of temperature. *Act Mater*. 2013;61(7):2460–2470.
- [20] Xu R, Liu Y, Sun F. Effect of isothermal aging on the microstructure, shear behavior and hardness of the Sn58Bi/Sn3.0Ag0.5Cu/Cu solder joints. *Results Phys*. 2019;15:102701.
- [21] Liu Y, Fu H, Zhang H, et al. Microstructure, hardness, and shear behavior of the as-soldered SnBi-SAC composite solder pastes. *J Mater Sci Mater Electron*. 2017;28:19113–19120.
- [22] Wu C, Shen J, Peng C. Effects of trace amounts of rare earth additions on the microstructures and interfacial reactions of Sn57Bi1Ag/Cu solder joints. *J Mater Sci Mater Electron*. 2012;23:14–21.
- [23] Hu F, Zhang Q, Jiang J, et al. Influences of Ag addition to Sn-58Bi solder on SnBi/Cu interfacial reaction. *Mater Lett*. 2018;214:142–145.